applied sciences

MDPI

Article

Gelatin-Enabled Microsensor for Pancreatic Trypsin Sensing

George Banis [1], Luke A. Beardslee [2] and Reza Ghodssi [1,2,*]

[1] Fischell Department of Bioengineering, University of Maryland, 2201 J.M. Patterson Hall, College Park, MD 20742, USA; gbanis@umd.edu

[2] Institute for Systems Research, University of Maryland, 2173 A.V. Williams Building, College Park, MD 20742, USA; labeardslee04@gmail.com

* Correspondence: ghodssi@umd.edu; Tel.: +1-301-405-8158

Received: 21 December 2017; Accepted: 28 January 2018; Published: 31 January 2018

Featured Application: Biosensors and bio-detection technologies.

Abstract: Digestive health is critically dependent on the secretion of enzymes from the exocrine pancreas to the duodenum via the pancreatic duct. Specifically, pancreatic trypsin is a major protease responsible for breaking down proteins for absorption in the small intestine. Gelatin-based hydrogels, deposited in the form of thin films, have been studied as potential sensor substrates that hydrolyze in the presence of trypsin. In this work, we (1) investigate gelatin as a sensing material; (2) develop a fabrication strategy for coating sensor surfaces; and (3) implement a miniaturized impedance platform for measuring activity levels of pancreatic trypsin. Using impedance spectroscopy, we evaluate gelatin's specificity and rate of degradation when exposed to a combination of pancreatic enzymes in neutral solution representative of the macromolecular heterogeneity present in the duodenal environment. Our findings suggest gelatin's preferential degradation to trypsin compared to enzymes such as lipase and amylase. We further observe their interference with trypsin behavior in equivalent concentrations, reducing film digestion by as much as 83% and 77%, respectively. We achieve film patterns in thicknesses ranging from 300–700 nm, which we coat over interdigitated finger electrode sensors. Finally, we test our sensors over several concentrations to emulate the range of pancreatic secretions. Ultimately, our microsensor will serve as the foundation for developing in situ sensors toward diagnosing pancreatic pathologies.

Keywords: gelatin; pancreas; impedance sensing; biomaterial films; biosensors; diagnostics

1. Introduction

Pancreatic trypsin is a protease essential to a functional digestive system, allowing for the breakdown of various proteins to enable nutritional absorption in the small intestine. It is secreted as the proenzyme trypsinogen by acinar cells, where it travels through the pancreatic duct into the duodenum and becomes activated upon hydrolysis by enterokinase on the lumen surface [1]. Lipase and α-amylase are among the other major enzymes that are activated in the duodenum. These enzymes enter the duodenum in a basic solution with the intent to neutralize the gastric acid entering from the stomach. In various types of pancreatic pathologies, such as chronic pancreatitis or pancreatic adenocarcinoma, trypsin activity has been shown to decrease, indicating the acinus or duct has been compromised in some way [2–4].

Current work on trypsin sensing involves substrate degradation in response to enzymolysis. The substrates range from cytochrome c to gelatin, albumin or poly-L-lysine, while transduction methods are equally variable, using either liquid crystal, fluorescence, ionic conductance, or resistance [5–9]. These substrates are chosen due to the type of bonds between their components,

as trypsin hydrolyzes specific peptide linkages that are formed from the amino acids lysine and arginine. Gelatin is a hydrolytic product of collagen, and the above amino acids consist of around 10–20% of most final gelatin forms [10]. Gelatin is also biocompatible, and therefore an attractive substrate material. As a hydrogel that begins as a low viscosity liquid, it can be formed to a variety of structures that are limited only by the tools used until it cools and transitions from sol to gel state.

One such structure is a thin film, common for various electronic sensors made from standard methods in monolithic fabrication. Deposition of hydrogel thin films has been achieved, while in the sol state, through strategies such as spin-coating, drop-casting, dip-coating, etc. [11]. Furthermore, crosslinking is utilized often to enhance the stability of the material, and is limited by the reactive functional groups in the structure's chemistry [12]. Glutaraldehyde, for example, has been used to allow for gelatin films to maintain structural integrity at higher temperatures [13,14]. Though it can be dangerous to cells, low concentrations do not significantly enhance toxicity. Most biochemical sensors for biomedical applications are not concerned with toxicity as they are often utilized in vitro, where the samples are either in buffer or fluids that have been removed from the body. Few sensing strategies are designed to operate in vivo, as there are significant risks associated when implementing foreign objects in the physiological environment, as well as sample complexity due to molecular heterogeneity in physiological fluids. When targeting trypsin, which, as discussed above, originates near the duodenum, regional sample heterogeneity, such as potential interfering species must be considered when performing sensor testing.

In this study, we developed and tested a sensing strategy for measuring trypsin activity in solutions containing several types of interfering enzymes characteristic of duodenal fluid. Crosslinked gelatin films were formed over interdigitated finger electrode (IDE) sensors, which were fabricated similarly to those described previously [15–17]. These sensors were inserted into fluidic chambers and exposed to various pancreatic enzymes while changes in the mass and impedance responses were recorded. Ultimately, it was possible to differentiate the presence of trypsin in each of these sensors and provide insight as to its role in producing complex impedimetric signals, offering potential for utilizing this method for in situ sampling.

2. Materials and Methods

2.1. IDE Sensor Fabrication and Film Deposition

Electrode patterns, consisting of one sensor for coating and one for negative control in devices 3 cm × 1 cm, were obtained through photolithography using standard process for NR9-1500PY photoresist over pyrex wafers. Cr/Au (15 nm/200 nm) was deposited via E-beam evaporation, followed by liftoff with acetone. Resulting IDE fingers, a total of 146, were 2 μm wide with 4 μm spacing and 960 μm length. Next, a 75 μm thick polyvinyl chloride (PVC) film (Semiconductor Equipment Corp, Moorpark, CA, USA) was applied to the wafer surface, and patterns were manually cut over one sensor per device. Gelatin type B from bovine skin (Sigma Aldrich, St. Louis, MO, USA) was added to 50 °C deionized (DI) water while stirring until complete dissolution to a final weight/volume of 5%. 200 μL gelatin solution was spin-coated at 400 rpm for 30 s over the sensors, then cooled overnight, forming over the test sensor. All gelatin films were crosslinked after overnight cooling with 0.5% glutaraldehyde solution in DI water at room temperature for at least 4 hours to improve thermal stability. After PVC removal from the IDE patterned wafer, gelatin film thicknesses were characterized with a profilometer (Veeco, Dektak-8 stylus, Plainview, NY, USA) ranging at 400–700 nm. IDE devices were then diced using a standard dicing saw (Microautomation, Centreville, VA, USA). After each experiment and analysis, the sensor dye were cleaned with 3:1 Piranha, tested, and reused using additional films that were drop-cast deposited and crosslinked over each dye, with one of the two sensors consistently covered with PVC. This process was done carefully to cover only one of the sensors on the devices to as to maintain the presence of a control sensor. The resulting films possessed thicknesses ranging from 60–90 μm.

2.2. Enzyme Solution Preparation

Trypsin from bovine pancreas (≥7500 benzoyl-L-arginine ethyl ester units/mg solid, 23.8 kDa), α-Amylase (≥10 units/mg solid, 51–54 kDa) and lipase (Type II, 100–500 units/mg protein, 48 kDa) from porcine pancreas, as well as phosphate-buffered saline (PBS) capsules were obtained from Sigma Aldrich. 0.1 M PBS (pH 7.4) was used in each experiment. Enzymes were mixed and incubated in PBS for at least 15 min at 37 °C before use. Trypsin solutions of either 1 or 0.5 mg/mL were used, while lipase and α-amylase were prepared at 1 mg/mL each. Heterogeneous solutions consisted of 1 mg/mL of each enzyme.

2.3. Impedance Sensing

Diced IDE devices were inserted into a custom two-piece 3D printed chambers containing an inlet and outlet. The parts were designed in SolidWorks (Dassault Systemes, Vélizy-Villacoublay, France) and printed from MED610 with an Objet30 Pro (Stratasys, Eden Prairie, MN, USA). Fluid was injected with syringe pumps at 20 µL/min through tygon tubing (Cole-Parmer, Vernon Hills, IL, USA) into the chamber inlet, then exited through the outlet into a waste beaker. Sensor response was recorded with each medium until signal saturation, beginning with air, PBS (negative control), then PBS with enzymes, described above. The chamber was incubated at ~37 °C for every experiment to simulate physiological temperature. IDE contact pads were connected to a CHI 660D Electrochemical workstation (CH Instruments, Bee Cave, TX, USA), one pad connected to the working terminal and the other pad to shorted reference and counter terminals. The AC current was swept from 10 Hz—1 MHz with potential amplitude of 50 mV every two minutes sequentially per sensor. Sensor substrates were weighed with a microbalance and profiled before deposition, after deposition once films were dehydrated, and after experimentation to determine absolute and loss of film mass.

2.4. QCM Sensing

As an additional means of verifying activity between the enzymes discussed above and the gelatin films, we investigated mass sensing using quartz crystal microbalance (Inficon, East Syracuse, NY, USA). For details on the specific methods and results obtained, see the Supplementary Materials (Section: QCM Methods and Results).

2.5. Image/Data Analysis

Films were observed and analyzed using an INM100 microscope (Leica, Wetzlar, Germany) and an S-3400 Variable Pressure Scanning Electron Microscope (SEM) (Hitachi, Tokyo, Japan). Impedance data were exported from CHI software as .txt files, and imported, along with film thickness profiles, into MatLAB (MathWorks, Natick, MA, USA) for analysis. Nyquist and Bode spectra were observed, and impedance at various frequencies were plotted over time for each condition.

3. Results

3.1. IDE Sensor and Film Structure and Morphology

Microscopic images of resulting IDE sensors, with and without spin-coated gelatin films before exposure to enzyme solutions, are displayed in Figure 1a. The gelatin films, depicted over the sensors on the left side of the image, were slightly frayed at the edges, but this did not directly affect sensor response as the edges were relatively distant from the IDEs. Figure 1b–d represent the same configuration, except after the sensor has been exposed to either PBS (b), trypsin (c), or all three enzymes (d) in PBS and has been dried. After surface profiling, it was evident that trypsin alone removes most the gelatin from the sensor surface, visualized in Figure 1c, while each other condition leaves a residue of film over the test sensor and more non-specific molecular adhesion to the control surface, such as the mixture-treated sensors depicted in Figure 1d. Table 1 describes the proportion of

remaining film thickness, mean values (n = 2), after exposure to each solution condition, calculated using Equation (1), where t is the thickness at each time point:

$$Film\ Thickness\ Remaining = \left(\frac{t_{pre-experiment} - t_{post-experiment}}{t_{pre-experiment}} \right) \quad (1)$$

A value of 1 would indicate no film was lost, and each thickness was achieved after signal saturation and complete drying in ambient environment.

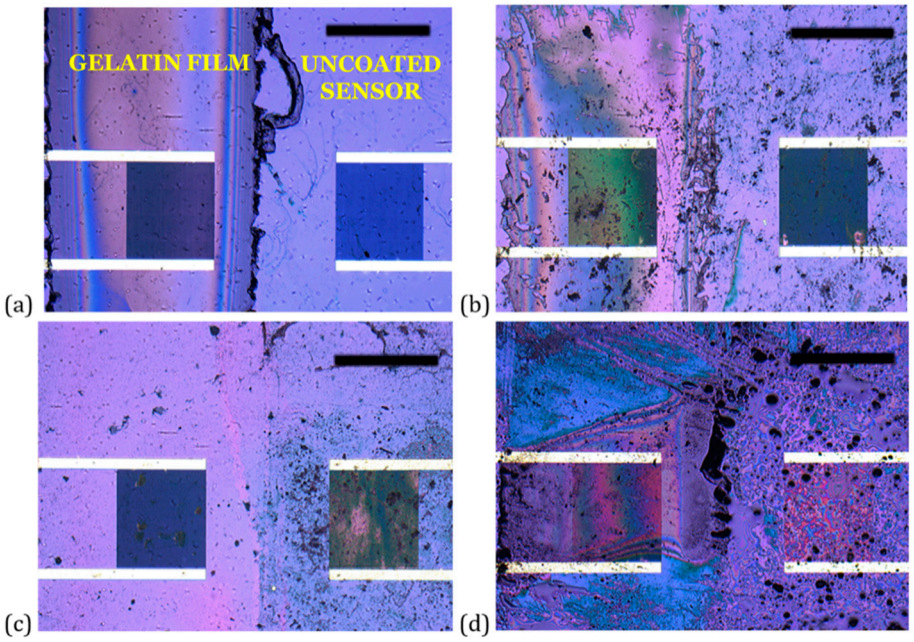

Figure 1. Resulting interdigitated finger electrode (IDE) sensors, with (**Left**) and without (**Right**) gelatin films, (**a**) pre-exposure to solutions, and post-exposure to (**b**) buffer; (**c**) trypsin; or (**d**) all three enzymes in buffer. Scale bar = 1 mm.

Table 1. Ratio of spin-coated film remaining after various enzyme conditions, analyzed with a contact profiler (n = 2).

Condition	Film Thickness Remaining (%)
PBS (Phosphate Buffered Saline)	78.6 ± 0.05
Amylase (1 mg/mL)	24.3 ± 0.08
Lipase (1 mg/mL)	52.4 ± 0.30
Trypsin (1 mg/mL)	11.1 ± 0.03
Trypsin (0.5 mg/mL)	21.7 ± 0.10

SEM images of the drop-cast films in various conditions can be viewed in Figure 2, where (a,b) are side-view and (c,d) are top-down. In Figure 2a, the surface of the dry, cross-linked films appears rough with an edge thickness of ~60 µm. After exposure to trypsin for several hours, at which the absolute impedance had saturated, the sensor was rinsed with DIH_2O and completely dried. The resulting edge thickness was then measured at ~9 µm, reflecting the removal of film as a result of hydrolysis from trypsin. The ratio of remaining film to the original is slightly less than 0.15, which is relatively consistent with the ratio of film remaining with the spin-coated film from Table 1 (0.13). Furthermore, the film is much smoother, and can be observed again from the top-view in Figure 2c.

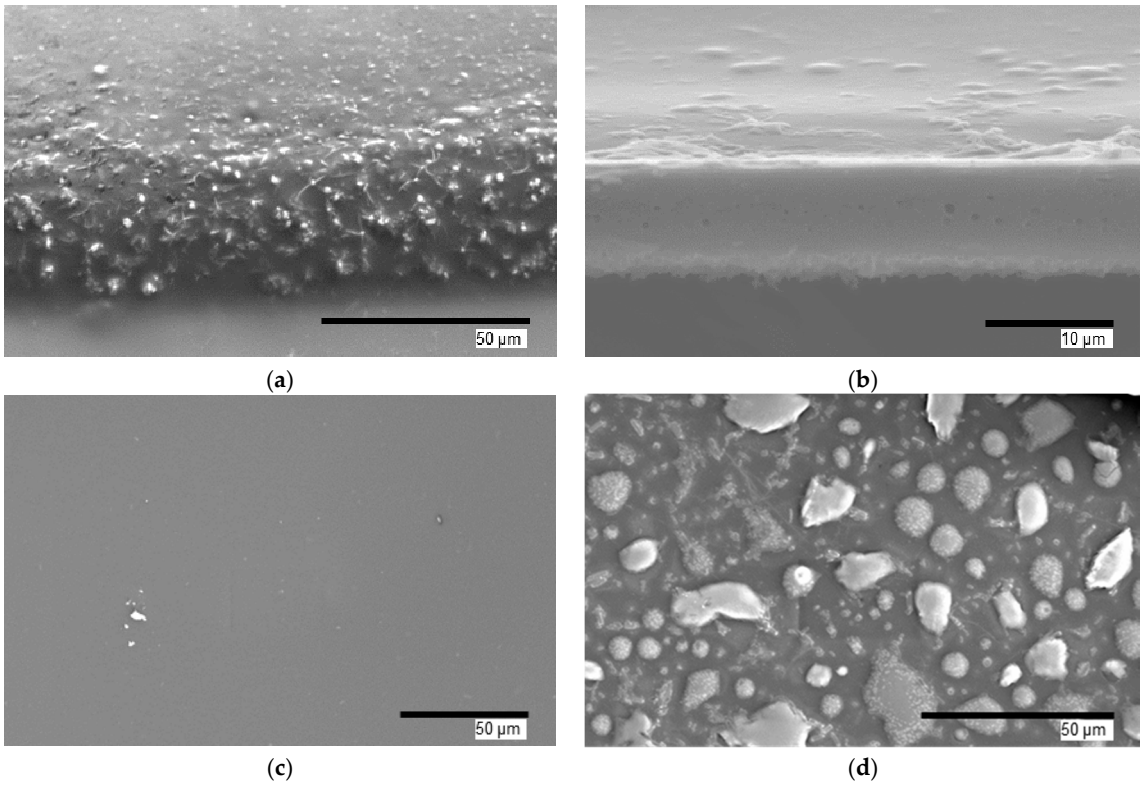

Figure 2. SEM of resulting drop-cast crosslinked gelatin films. Edge views of film (**a**) without exposure to enzyme solutions and (**b**) after exposure to trypsin, and top views of film (**c**) after exposure to trypsin and (**d**) after exposure to all three enzymes in buffer.

After the film was exposed to all three enzymes, however, the thickness reduced to only ~0.68 of the original film after the impedance signal had saturated. This indicates saturation occurred before even half of the film had been degraded. Further, as depicted in Figure 2d, globules form in the film, some of which can exceed 15 µm in diameter. This is likely due to the entrapment of non-specific enzymes in the gelatin matrix, possibly due to residue glutaraldehyde within the film, and possibly responsible for attenuating the peptide cleavage by trypsin [18–20]. Further, the immobilization of the non-specific enzymes in the gelatin may induce tighter bonds (i.e., aldimine with the amylase) to form, possibly explaining the decrease in thickness by them alone [21]. However, based on the results in Table 1, there is still less degradation with all three enzymes than what occurs with only amylase or lipase, suggesting enzymatic cross-interference in the solution before interactions occur at the gelatin surface. Due to the prevalence of arginine and lysine in the amino acid compositions of both amylase and lipase, trypsin may be performing additional proteolysis on the nonspecific enzymes in the solution as a result [22,23].

3.2. Trypsin Impedance Results

Impedance spectra were recorded after film stabilization under PBS flow with a 3D-printed setup. The absolute impedance at 10 kHz revealed to be most sensitive to the presence of trypsin during flow due to the largest changes that occurred relative to the initial signal saturation. Figure 3 presents data comparing the effect of different concentrations of trypsin, which show that 0.5 mg/mL trypsin reduced the film ΔZ rate to 0.114 kΩ/min, a significant drop compared to the 2.88 kΩ/min rate of the 1 mg/mL concentration. The curve for "Trypsin—No Film" essentially represents the impedance of PBS over the sensor since trypsin is not significantly polar and thus does not alter the dielectric properties of the buffer, while "Control—Film" represents the impedance of the film after equilibrating with the PBS.

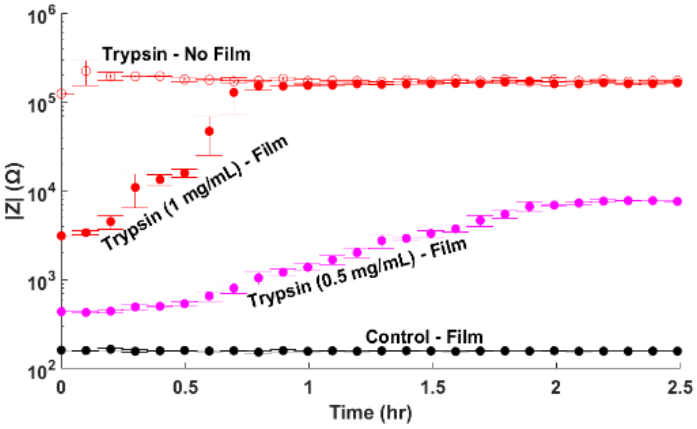

Figure 3. Representative impedance responses at 10 kHz of sensors, either uncoated or coated with a gelatin film, to trypsin at 1 (both film and no film), 0.5 (film only) and 0 mg/mL in phosphate-buffered saline (Control). The error bars plot the temporal change in impedance at respective time points (span = 3).

Interestingly, the impedance of the film alone is expected to be higher than that of PBS due to the gelatin's relatively neutral isoelectric point [24]. It is likely, however, that equilibration with the PBS flow allowed salt ions to accumulate, thereby increasing the ion concentration in the gelatin matrix over the sensor.

In Figure 4, we report a representative sequence of Bode plots at different exposure times that convey changes in the electronic properties of equivalent circuit models, such as the double-layer capacitance and solution resistance.

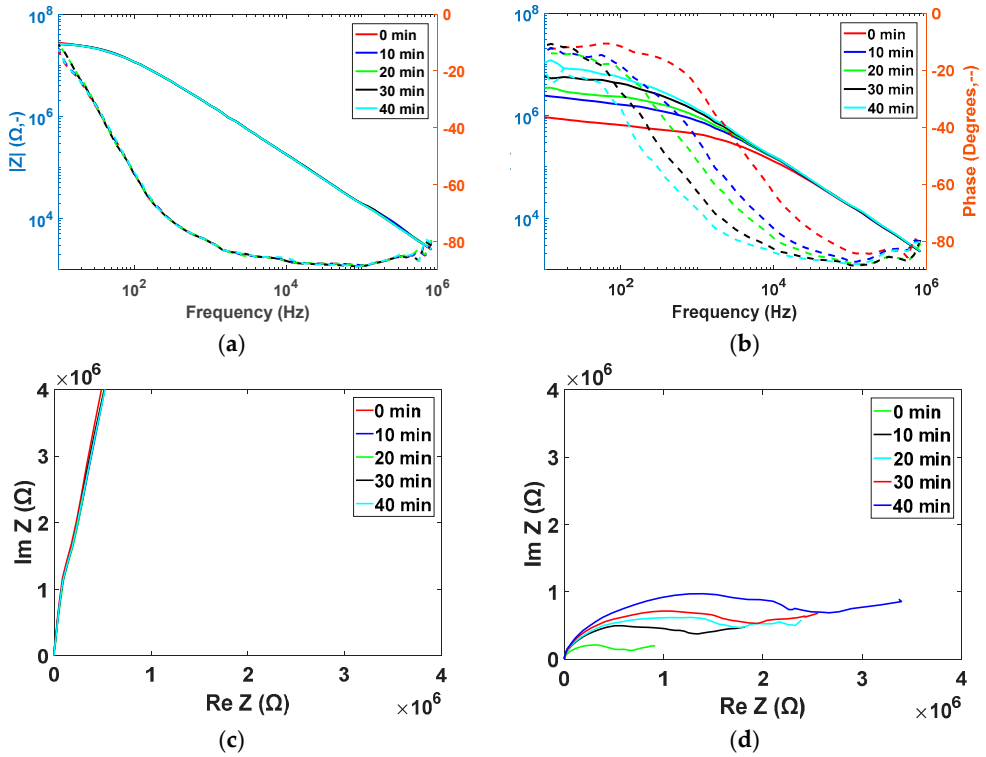

Figure 4. Representative bode and Nyquist plots for progressive exposure of (**a**,**c**) uncoated and (**b**,**d**) gelatin-coated sensors to 1 mg/mL trypsin in buffer. Solid (-) and dotted (–) lines indicate |Z| and the phase, respectively.

Here, we see over time, both the phase and impedance spectra of the coated sensor approach those of the uncoated sensor, indicating a decrease in film coverage that reflects trypsin degradation of the film due to increased exposure of the sensors to the buffer. We also observe an increase in the frequency range possessing a phase approaching 90°, further evidence that capacitive elements become more dominating in the circuit. Additionally, there is an increase in the charge-transfer resistance (R_{CT}) in the Nyquist plot, illustrated by the increase in diameter of the semicircles (Figure 4d) as trypsin continues to remove film from the sensor surface. This is opposite to what is observed in uncoated sensors (Figure 4c), which further supports the likelihood of ion accumulation in the film.

3.3. Enzyme Mixture Impedance Results

After understanding the impact of trypsin on the impedance of the film-coated sensors compared to the uncoated ones, we then observed how introducing non-specific enzymes to the solution would alter this effect. In Figure 5a, we observe that the addition of amylase and lipase caused a significant decrease in rate of ΔZ when added to trypsin, measured at 6.77×10^{-4} kΩ/min. Further, when amylase or lipase are alone in buffer, we observe the trend of decreasing impedance, opposite to the trend observed with trypsin alone. The origin of the increase in impedance during the first hour of the sensors exposed to lipase.

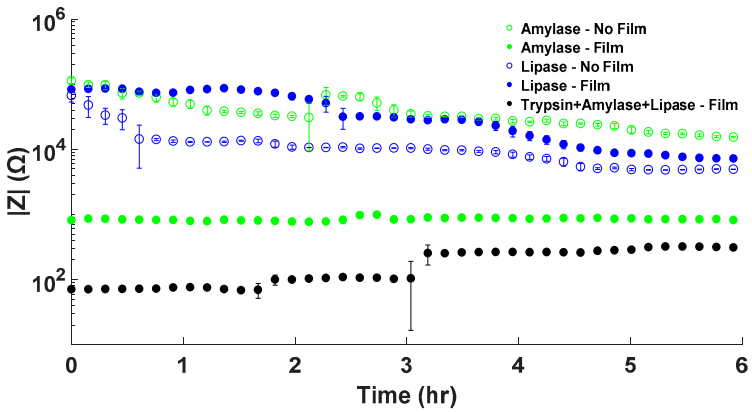

Figure 5. Representative impedance responses at 10 kHz of sensors, either uncoated or coated with a gelatin film, to trypsin, amylase, or lipase, each at 1 mg/mL, or combinations of each enzyme with trypsin. The error bars plot the temporal change in impedance at respective time points (span = 3).

Upon Nyquist plot analysis of non-specific enzyme impact (Figure 6), we observe additional trends, opposite again to those from trypsin, induced by amylase and lipase. These trends include a decrease in both the 45° tail (representative of the Warburg impedance Z_W) and the radius of the semicircular region (representative of the R_{CT}), the latter of which indicates the lack of ion diffusion into the media to account for the increase in exchange current density (i_O) according to Equation (2):

$$R_{CT} = \frac{RT}{nFi_O} \tag{2}$$

where R is the gas constant, T is the temperature, n is the number of electrons, and F is Faraday's constant [25]. This effect on the R_{CT} can be a result of the lack of film degradation, or even increase in film thickness [26]. The semi-circular region in the film responding to amylase or lipase is much more defined, indicating a larger double-layer capacitance of the active material, i.e., the film and its constituents. This characteristic of the film is also maintained while there is buffer alone, suggesting the non-specific enzymes do not significantly affect the structure of the film in the absence of trypsin. Alternatively, in the case of most nonspecific enzymes, residual glutaraldehyde remaining in the film may have allowed for accumulation of additional α-amylase or lipase, likely observed in

Section 3.1 [18–20]. Upon measuring the film after exposure to all three enzymes, we see the similar trend of increasing impedance as when trypsin is alone, though at a much slower pace. We again observe the phenomena of decreasing R_{CT} in the Nyquist plot, similarly to what occurred with the amylase and lipase alone. The 4-fold reduction in degradation rate may be alleviated by modifying the film to prevent non-specific binding, such as with the use alternative crosslinkers (microbial transglutaminase has shown to be effective), inhibitors (orlistat or tendamistat for lipase and amylase, respectively) or with more specific film materials to trypsin (i.e., poly-L-lysine) [27–29]. Overall, however, the experiments conducted above allowed us to observe the impacts of these enzymes on the impedance of these gelatin films, and it appeared that the presence of trypsin, rather than the non-specific enzymes, is responsible for inducing these changes in impedance over the film-coated sensors.

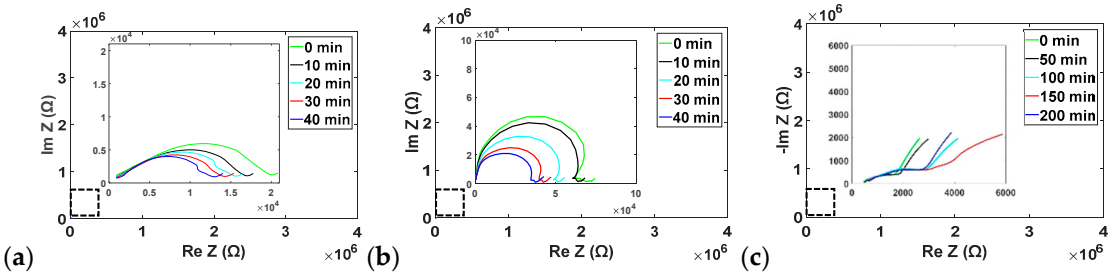

Figure 6. Representative Nyquist plots for gelatin-coated sensors to (**a**) 1 mg/mL lipase; (**b**) 1 mg/mL amylase; and (**c**) trypsin, amylase, and lipase, each at 1 mg/mL over time.

4. Conclusions

This work demonstrates an impedance-based sensing strategy for measuring film-degradation using gelatin as a substrate for pancreatic trypsin. While sensor fabrication proved relatively straightforward, the information obtained offered broad insight as to enzymatic interactions that occur between the film and various species in the media. We observed linearity in rate of impedance change over time by measuring the degradation rate of gelatin films by trypsin, and that nonspecific enzymes diminish this effect by nearly 4-fold. The changes in impedance resulting from changes in film morphology are likely to translate to similar film and enzyme-targeting combinations, and may suggest potential strategies that should be implemented when measuring in more complex environments such as pancreatic secretions in vivo.

Supplementary Materials: The following are available online at www.mdpi.com/2076-3417/8/2/208/s1, QCM Methods and Results.

Acknowledgments: This work was supported by the National Science Foundation ECCS Program under Award 1738211. The authors acknowledge the support from the Maryland NanoCenter and its FabLab.

Author Contributions: G.B. and L.A.B. conceived and designed the experiments and analyzed the data; G.B. performed the experiments; R.G. contributed reagents/materials/analysis tools; G.B. wrote the paper.

Conflicts of Interest: The founding sponsors had no role in the design of the study; in the collection, analyses, or interpretation of data; in the writing of the manuscript, and in the decision to publish the results.

References

1. Pandol, S.J. The Exocrine Pancreas. *Morgan Claypool Life Sci.* **2010**. [CrossRef] [PubMed]
2. Raimondo, M.; Imoto, M.; Dimagno, E.P. Rapid endoscopic secretin stimulation test and discrimination of chronic pancreatitis and pancreatic cancer from disease controls. *Clin. Gastroenterol. Hepatol.* **2003**, *1*, 397–403. [CrossRef]
3. Goldberg, D.M.; Wormsley, K.G. The interrelationships of pancreatic enzymes in human duodenal aspirate. *Gut* **1970**, *11*, 859–866. [CrossRef] [PubMed]
4. James, O. The Lundh test. *Gut* **1973**, *14*, 582–591. [CrossRef] [PubMed]

5. Chuang, C.-H.; Lin, Y.-C.; Chen, W.-L.; Chen, Y.-H.; Chen, Y.-X.; Chen, C.-M.; Shiu, H.W.; Chang, L.-Y.; Chen, C.-H.; Chen, C.-H. Detecting trypsin at liquid crystal/aqueous interface by using surface-immobilized bovine serum albumin. *Biosens. Bioelectron.* **2016**, *78*, 213–220. [CrossRef] [PubMed]
6. Zhang, L.; Qin, H.; Cui, W.; Zhou, Y.; Du, J. Label–free, turn–on fluorescent sensor for trypsin activity assay and inhibitor screening. *Talanta* **2016**, *161*, 535–540. [CrossRef] [PubMed]
7. Neff, P.A.; Serr, A.; Wunderlich, B.K.; Bausch, A.R. Label-Free Electrical Determination of Trypsin Activity by a Silicon-on-Insulator Based Thin Film Resistor. *ChemPhysChem* **2007**, *8*, 2133–2137. [CrossRef] [PubMed]
8. Duan, C.; Alibakhshi, M.A.; Kim, D.-K.; Brown, C.M.; Craik, C.S.; Majumdar, A. Label-Free Electrical Detection of Enzymatic Reactions in Nanochannels. *ACS Nano* **2016**, *10*, 7476–7484. [CrossRef] [PubMed]
9. Stoytcheva, M.; Zlatev, R.; Cosnier, S.; Arredondo, M.; Valdez, B. High sensitive trypsin activity evaluation applying a nanostructured QCM-sensor. *Biosens. Bioelectron.* **2013**, *41*, 862–866. [CrossRef] [PubMed]
10. Eastoe, J.E. The amino acid composition of mammalian collagen and gelatin. *Biochem. J.* **1955**, *61*, 589. [CrossRef] [PubMed]
11. Li, M. Thin Films of Stimuli-Responsive Hydrogels. Ph.D. Thesis, Université Pierre et Marie Curie-Paris VI, Paris, France, 18 June 2015.
12. Yeo, Y.; Geng, W.; Ito, T.; Kohane, D.S.; Burdick, J.A.; Radisic, M. Photocrosslinkable hydrogel for myocyte cell culture and injection. *J. Biomed. Mater. Res. B Appl. Biomater.* **2007**, *81*, 312–322. [CrossRef] [PubMed]
13. Schyrr, B.; Boder-Pasche, S.; Ischer, R.; Smajda, R.; Voirin, G. Fiber-optic protease sensor based on the degradation of thin gelatin films. *Sens. Biosens. Res.* **2015**, *3*, 65–73. [CrossRef]
14. Bigi, A.; Cojazzi, G.; Panzavolta, S.; Rubini, K.; Roveri, N. Mechanical and thermal properties of gelatin films at different degrees of glutaraldehyde crosslinking. *Biomaterials* **2001**, *22*, 763–768. [CrossRef]
15. Zang, F.; Gerasopoulos, K.; Fan, X.Z.; Brown, A.D.; Culver, J.N.; Ghodssi, R. Real-time monitoring of macromolecular biosensing probe self-assembly and on-chip ELISA using impedimetric microsensors. *Biosens. Bioelectron.* **2016**, *81*, 401–407. [CrossRef] [PubMed]
16. Kim, Y.W.; Meyer, M.T.; Berkovich, A.; Subramanian, S.; Iliadis, A.A.; Bentley, W.E.; Ghodssi, R. A surface acoustic wave biofilm sensor integrated with a treatment method based on the bioelectric effect. *Sens. Actuators Phys.* **2016**, *238*, 140–149. [CrossRef]
17. Kim, Y.W.; Sardari, S.E.; Meyer, M.T.; Iliadis, A.A.; Wu, H.C.; Bentley, W.E.; Ghodssi, R. An ALD aluminum oxide passivated Surface Acoustic Wave sensor for early biofilm detection. *Sens. Actuators B Chem.* **2012**, *163*, 136–145. [CrossRef]
18. Jaiswal, N.; Prakash, O.; Talat, M.; Hasan, S.H.; Pandey, R.K. α-Amylase immobilization on gelatin: Optimization of process variables. *J. Genet. Eng. Biotechnol.* **2012**, *10*, 161–167. [CrossRef]
19. Alteriis, E.D.; Parascandola, P.; Salvadore, S.; Scardi, V. Enzyme immobilisation within insolubilised gelatin. *J. Chem. Technol. Biotechnol. Biotechnol.* **1985**, *35*, 60–64. [CrossRef]
20. Fadnavis, N.W.; Sheelu, G.; Kumar, B.M.; Bhalerao, M.U.; Deshpande, A.A. Gelatin Blends with Alginate: Gels for Lipase Immobilization and Purification. *Biotechnol. Prog.* **2003**, *19*, 557–564. [CrossRef] [PubMed]
21. Jaiswal, N.; Prakash, O. Immobilization of Soybean α-amylase on Gelatin and its Application as a Detergent Additive. *Asian J. Biochem.* **2011**, *6*, 337–346. [CrossRef]
22. Caldwell, M.L.; Dickey, E.S.; Hanrahan, V.M.; Kung, H.C.; Kung, J.T.; Misko, M. Amino Acid Composition of Crystalline Pancreatic Amylase from Swine1. *J. Am. Chem. Soc.* **1954**, *76*, 143–147. [CrossRef]
23. Bianchetta, J.D.; Bidaud, J.; Guidoni, A.A.; Bonicel, J.J.; Rovery, M. Porcine Pancreatic Lipase. *Eur. J. Biochem.* **1979**, *97*, 395–405. [CrossRef] [PubMed]
24. Thimann, K.V. The Effect of Salts on the Ionisation of Gelatin. *J. Gen. Physiol.* **1930**, *14*, 215–222. [CrossRef] [PubMed]
25. Barsoukov, E.; Macdonald, R. *Impedance Spectroscopy: Theory, Experiment, and Applications*, 2nd ed.; Wiley: Hoboken, NJ, USA, 2005.
26. Daniels, J.S.; Pourmand, N. Label-Free Impedance Biosensors: Opportunities and Challenges. *Electroanalysis* **2007**, *19*, 1239–1257. [CrossRef] [PubMed]
27. Erwanto, Y.; Kawahara, S.; Katayama, K.; Takenoyama, S.; Fujino, H.; Yamauchi, K.; Morishita, T.; Kai, Y.; Watanabe, S.; Muguruma, M. Microbial Transglutaminase Modifies Gel Properties of Porcine Collagen. *Asian-Australas. J. Anim. Sci.* **2003**, *16*, 269–276. [CrossRef]

28. Franson, K.; Rössner, S. Fat intake and food choices during weight reduction with diet, behavioural modification and a lipase inhibitor. *J. Intern. Med.* **2000**, *247*, 607–614. [CrossRef] [PubMed]
29. Konig, V.; Vertesy, L.; Schneider, T.R. Structure of the alpha-amylase inhibitor tendamistat at 0.93 A. *Acta Crystallogr.* **2003**, *59*, 1737–1743.